Supporting Information

Influences of alkyl side-chain length on the carrier mobility in organic semiconductors: herringbone vs. pi-pi stacking

Zhiying Ma, Hua Geng, Dong Wang and Zhigang Shuai

1. The effect of D3(BJ) on the intra-molecular interaction

For evaluating the effect of dispersion correction together with the Becke-Johnson damping function on the intra-molecular interaction, the reorganization energies of all compounds with alkyl chains from adiabatic potential-energy surfaces have also evaluated using both (dispersion-uncorrected) B3LYP and (dispersion correction together with the Becke-Johnson damping function)[1] B3LYP-D3(BJ) in combination with 6-31G* basis set.

As presented in Table S1, the results from the normal mode analyses and the adiabatic potential-energy surfaces are consistent and the reorganization energies are not affected by adding D3 dispersion correction together with Becke-Johnson damping function.

Table S1 The calculated internal reorganization energies (RE).

Complexes	RE (meV)[a]	RE (meV)[b]	RE (meV)[c]
NDI-C0	332	329	327
NDI-C4	351	351	347
NDI-C5	350	349	347
NDI-C6	351	350	347
NDI-C12	350	349	347
NDI-C14	350	349	347
BTBT-C0	228	226	224
BTBT-C8	246	244	246
BTBT-C10	246	244	247
BTBT-C12	252	245	247
BSBS-C0	200	198	198
BSBS-C8	227	225	228
BSBS-C10	226	224	226
BSBS-C12	226	224	226
BSBS-C14	227	224	227

[a] The reorganization energies are obtained from the normal mode analyses at the B3LYP/6-31G(d) level of theory.
[b] The reorganization energies are obtained from the adiabatic potential-energy surfaces at the B3LYP/6-31G(d) level of theory
[c] The reorganization energies are obtained from the adiabatic potential-energy surfaces at the B3LYP-D3(BJ)/6-31G(d) level of theory.

2. The properties of the non-substituted aromatics.

The π-conjugated backbone with no alkyl chain substituents (i.e. **NDI-C0**, **BTBT-C0**, **BSBS-C0**) have also calculated for comparison. From Table 1 and S2, it is obvious that the HOMO (or LUMO) energy level, AEA (or AIP), reorganization energy of the systems with alkyl chains are shifted slightly compared with that of the π-conjugated backbone with no alkyl chain substituents, which is ascribe to the weak electron-donating properties of alkyl chains.

Compared with the systems presenting in Figure 4, **NDI-C0** shown in Figure S1 also adopts the π-π stacking configuration and displays three-dimensional transport behaviour, while there is an angle between the molecules in the dimer (take **P1** pathway as an example, seen from the Fig. S2). This difference between

the systems with alkyl chain and no alkyl chain should ascribe to the variation of their geometric structures, since the introduction of alkyl chain changes their interaction positions between molecules in packing process. As presented in Table S3, Figure S1 and Table 2, the largest absolute values of transfer integrals for **NDI-C0** is along **P9** and **P10** pathways, which are less than those for **NDI-C6** and larger than those for **NDI-C12**. While there are more pathways possessing large transfer integrals to transfer charge for **NDI-C0**.

Moreover, compared with the systems with alkyl chains, **BTBT-C0** and **BSBS-C0** also adopt herringbone stacking configuration and display two-dimensional transport behavior as illustrated in Fig. S1. And the absolute values of transfer integrals along π stacking **P1** and **P2** are also much larger than the other pathways as collected in Table S3. On the other hand, the absolute values of transfer integral along the π stacking pathways for **BTBT-C0** are similar with those for **BTBT-C12** and larger than those for **BTBT-C8** and **BTBT-C10** (seen from Table S3 and Table 5). While for the directions along herringbone stacking, the absolute values of **BTBT-C0** are lower than those of **BTBT-C12**, which suggests that the former possesses a strong anisotropy of charge mobility. The absolute values of transfer integrals along the π stacking pathways for **BSBS-C0** are between those for **BSBS-C8** and those for **BSBS-C12**. These discussions suggest that the introduction of alkyl chains don't have to enhance charge transfer.

Last, the charge mobility of the π-conjugated backbone with no alkyl chain substituents is simulated and collected in Table S4. As illustrated in Fig. 8 and Table S4, the three-dimensional average electron mobility of **NDI-C0** is only lower than that of **NDI-C4**. For the herringbone stacking systems, the mobilities of **BTBT-C0** and **BSBS-C0** are lower than those of the π-conjugated backbone with the longest alkyl chain, i.e. **BTBT-C12** and **BSBS-C12**, respectively.

Table S2 The calculated LUMOs, HOMOs, adiabatic electron affinities (AEA), adiabatic ionization potentials (AIP), and internal reorganization energies (RE).

Complexes	LUMO (eV)[a]	HOMO (eV)[a]	AEA (eV)[a]	AIP (eV)[a]	RE (meV)[b]
NDI-C0	-3.96	-7.56	2.63		332
BTBT-C0	-1.59	-5.83		7.23	228
BSBS-C0	-1.63	-5.73		7.15	200

[a] The values are obtained at the B3LYP/6-31+G(d)//B3LYP/6-31G(d) level.
[b] The reorganization energies are obtained from the normal mode analyses.

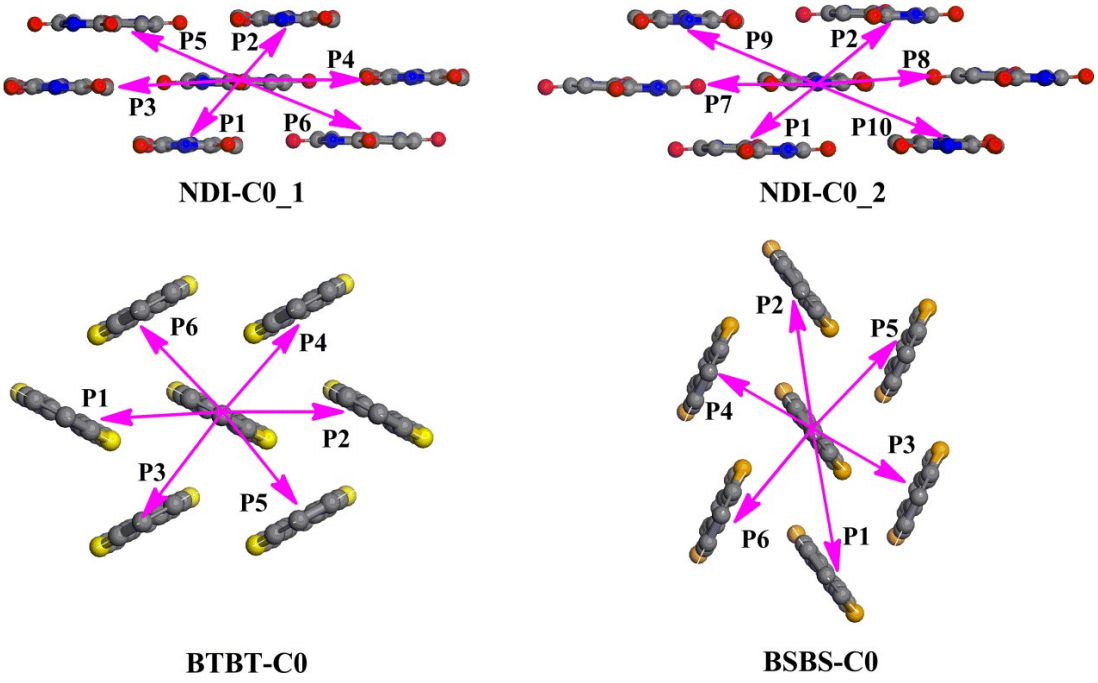

Fig. S1 Schematic illustration of charge hopping pathways for **NDI-C0**, **BTBT-C0**, and **BSBS-C0**.

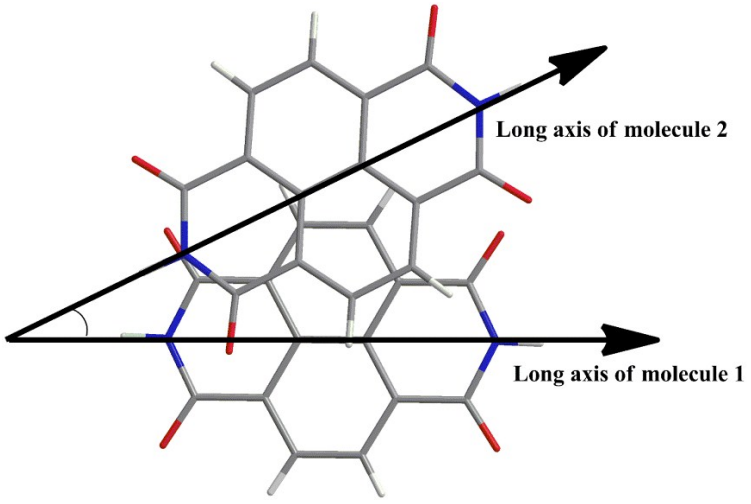

Fig. S2 The top view of the dimer along **P1** pathway.

Table S3. The transfer integrals (V, in meV) and intermolecular distances between the centroids of the dimer (d_C, in Å) along major hopping pathways selected based on the crystal structures.

	NDI-C0	**BTBT-C0**	**BSBS-C0**

	d_C	V	d_C	V	d_C	V
P1	4.491	34	5.862	54	6.025	86
P2	4.491	34	5.862	54	6.025	86
P3	9.347	-16	4.932	-14	5.177	-28
P4	9.347	-16	4.932	-14	5.177	-28
P5	8.196	-40	4.932	-14	5.177	-28
P6	8.196	-40	4.932	-14	5.177	-28
P7	9.978	-6				
P8	9.978	-6				
P9	7.629	58				
P10	7.629	58				

Table S4. The calculated mobilities of **NDI-C0**, **BTBT-C0**, and **BSBS-C0**

Complexes	Mobility
NDI-C0	5.76
BTBT-C0	3.57
BSBS-C0	12.32

1 S. Grimme, S. Ehrlich and L. Goerigk, *J. Comput. Chem.*, 2011, **32**, 1456–1465.